New low temperature multiphase ferroelectric films

Eric Bescher, Yuhuan Xu, and J. D. Mackenzie
Department of Materials Science and Engineering, University of California Los Angeles, Los Angeles, California 90095-1595

(Received 23 June 2000; accepted for publication 16 February 2001)

This article describes the low-temperature synthesis of new multiphase ferroelectrics containing an inorganic ferroelectric phase entrapped in amorphous silica or in an organically modified silicate (ormosil). Sol gel derived $LiNbO_3$ and $BaTiO_3$ crystals were grown in SiO_2 and in $RSiO_{1.5}$ glass where R contains a chromophore (TDP) insensitive to hydrolysis and condensation reactions. The $LiNbO_3-SiO_2$ and $BaTiO_3-SiO_2$ compositions as well as the TDP–$LiNbO_3-SiO_2$ and TDP–$BaTiO_3-SiO_2$ ormosils exhibit ferroelectric-like properties. This unusual characteristic is due to the presence of small, partially ordered crystallites of the ferroelectric, dispersed in the amorphous matrix. In addition to their ferroelectric properties, the ormosils also exhibit interesting optical characteristics: the TDP–$BaTiO_3-SiO_2$ materials are red, whereas the TDP–$LiNbO_3-SiO_2$ are yellow. The materials described in this article are representative of two new classes of weak ferroelectrics. In the first class, a ferroelectric is dispersed in an amorphous matrix. The second class may be called ''organically-modified crystals'': small ferroelectric crystals embedded in an organically modified matrix. The fabrication of such materials is possible for inorganic crystalline phases forming at temperatures below the decomposition temperature of the organic (about 250 °C). This article also contains some theoretical considerations explaining why these materials, although amorphous by x-ray diffraction, exhibit ferroelectric-like properties. © *2001 American Institute of Physics.* [DOI: 10.1063/1.1364647]

I. INTRODUCTION

The sol–gel method has been widely utilized to prepare both oxide glasses such as silica and silicates and crystalline oxides such as alumina and titania. When the starting liquid solution solidifies, the gel formed is invariably a porous amorphous solid, regardless of chemical composition. After drying and heating to higher temperatures, one type of oxide system will give a solid dense glass whereas another type will give a crystalline material. The tendency towards glass formation or crystallization from an amorphous gel is governed primarily by the coordination number of the cations. It has been shown that the Zachariasen rules for melt-formed glasses are applicable also to gel-derived glasses. It is relatively easy to obtain a ferroelectric crystal such as $BaTiO_3$ by heating an amorphous oxide gel containing the appropriate cations in the proper ratios.[1] Indeed, many ferroelectric materials have been made by the sol–gel method, including single crystal films.[2–4] For the synthesis of single crystals in particular, the use of ''double alkoxides'' is preferred. The reason is that the most important chemical bonds such as Ba–O–Ti in the case of $BaTiO_3$ are already present in the precursor. This would facilitate the growth of $BaTiO_3$ crystals when the amorphous gel is heated. Recently, through the use of such double alkoxides, we discovered that a $LiNbO_3$ gel although still amorphous by x-ray diffraction, exhibited ferroelectric-like behavior.[5] Careful electron microscopy revealed the presence of extremely small (a few tens of Å) $LiNbO_3$ crystallites which were named ''ferrons.'' Ferroelectric behavior can be ascribed to the interaction of ferrons through the distorted NbO_6 of the amorphous matrix. This led to this study of some new multiphase inorganic materials such as $LiNbO_3$ ferrons dispersed in a silica matrix. Also, optically active phases were incorporated into the $LiNbO_3$-silica phase to give a new family of inorganic–organic hybrid materials. Many of these new multiphase materials have been prepared in the form of thin films and shown to exhibit ferroelectric-like behavior.[6] The objectives of this article are to present a summary of the preparation, ferroelectric properties, and current theoretical understanding of these new multiphase ferroelectric materials which can be fabricated in the form of thin films at low temperatures. It should also be noted that traditional ferroelectric glass ceramics are well known, and require high processing temperatures. They are not amenable to the kind of organic modification we are exploring in this study.

II. PREPARATION METHODS

$BaTiO_3-SiO_2$ films where fabricated by stirring tetraethylorthosilicate (TEOS) (99.99%) from Aldrich Chemicals with barium–titanium methoxyethoxide from Gelest Inc. (Tullytown, PA) for 30 min in air prior to spin coating. $LiNbO_3-SiO_2$ films where fabricated using TEOS (99.99%) from Aldrich Chemicals and lithium–niobium methoxyethoxide from Gelest Inc. The $BaTiO_3/SiO_2$ and $LiNbO_3/SiO_2$ molar ratio was 1 for all samples. The temperature programed desorption (TDP) (Fig. 1) was also obtained from Gelest Inc. The organically modified ferroelectrics were investigated using samples of molar composition 45TDP–45$BaTiO_3$–10SiO_2, and 45TDP–45$LiNbO_3$–

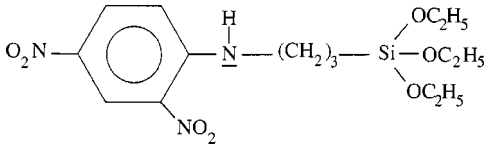

FIG. 1. 3-N-(3-triethoxysilylpropyl) 2,4 dinitrophenylamine.

$10SiO_2$. Hence, the TDP/metal oxide molar ratio was 1 for all samples. The 10% mole. SiO_2 was used to provide cross linking with the TDP.

TDP was first hydrolyzed in acetone ([Acetone]/[TDP]=20) with water at pH=1 ([H_2O]/[TDP]=2) for 30 min prior to addition of the TEOS and the Li–Nb or Ba–Ti alkoxide. The solution was then stirred for another 30 min. For transmission electron microscopy (TEM) characterization, thick films were made by pouring an appropriate amount of solution on a glass slide, and using the cracked-up materials for various heat-treatment temperatures, up to 800 °C for inorganic samples, up to 200 °C for organic–inorganic samples. For optical characterization, the films were fabricated by spin coating onto quartz. For dielectric and ferroelectric characterization, films were spun on highly doped silicon substrates. The films were then fired at the desired temperatures in air, and a 4000 Å thick gold coating was sputtered onto the film using a mask. Polarization–electric (P–E) loops were measured using a standard bridge setup described in a previous paper.[7] The thickness of the films was measured using a Dektak profilometer. UV-visible spectra were measured on a Hewlett-Packard spectrophotometer HP 8452.

III. EXPERIMENTAL RESULTS

A. Ferroelectric properties

$LiNbO_3-SiO_2$ and $BaTiO_3-SiO_2$, fired as low as 200 °C, exhibit polarization–electric field (P–E) loops as shown in Fig. 2. In order to establish with certainty that the loops were not spurious, a control experiment had been carried out. For this control experiment, a field was applied to a highly doped silicon wafer on which a thin (~500 Å) layer of SiO_2 had been deposited by the sol–gel process, and subsequently coated with gold. No P–E loop was observed for this material, indicating therefore that the neither the amorphous SiO_2 matrix, nor junction effects were responsible for the loops observed for $LiNbO_3-SiO_2$ or $BaTiO_3-SiO_2$.

The P–E loops in themselves prove that permanent, reversible dipoles are present in the material, and the remanent polarization P_r shows that such dipoles interact with each other to spontaneously align even in the absence of an applied external field. The values obtained from the experiments are V_c and V_s, as described in Ref. 7. For the $LiNbO_3/SiO_2$ sample, we obtained $E_c=0.54\,\mathrm{kV\,cm}\,1$ and $P_s=0.15\,\mu\mathrm{C\,cm}^2$. For the $BaTiO_3/SiO_2$ sample, the measured values were $P_r=0.24\,\mu\mathrm{C\,cm}^{-2}$ and $E_c=8.74\,\mathrm{kV\,cm}^{-1}$.

The P_r value for single crystal $LiNbO_3$ are reported to be between 40–70 $\mu\mathrm{C\,cm}^{-2}$, and for amorphous sol–gel derived $LiNbO_3$, about 5 $\mu\mathrm{C\,cm}^{-2}$. The values obtained for our

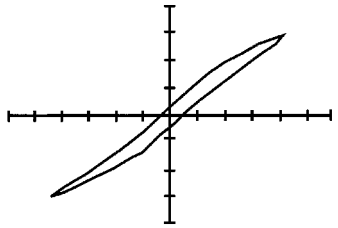

x-axis: E 2.72 kV.cm^{-1} per division
y- axis: P 0.10 μC cm^{-2} per division
50%$LiNbO_3$-50% SiO_2 heat-treated at 200°C for 2 hours

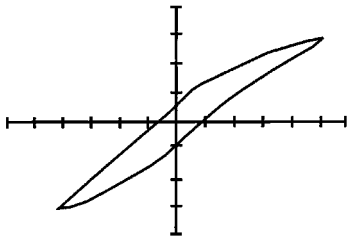

x-axis: E 2.91 kV.cm^{-1} per division
y- axis: P 0.06 μC cm^{-2} per division
50%$BaTiO_3$-50% SiO_2 heat-treated at 200°C for 2 hours

FIG. 2. P–E loops in $LiNbO_3-SiO_2$ and $BaTiO_3-SiO_2$ heat treated at 200 °C 2 h.

materials are therefore smaller but reasonable, considering that $LiNbO_3$ is mixed with SiO_2. The coercive field for $BatiO_3$ single crystal is 1 kV/cm^{-1}, and increases to about 5 $\mathrm{kV\,cm}^{-1}$ for a high quality $BaTiO_3$ polycrystalline ceramic. The values obtained here are therefore higher, which is a reflection of the higher complexity of the system (perhaps due to surface effects or porosity), but on the order of magnitude of results obtained for sol-gel derived stoichiometric $BaTiO_3$ ($E_c=10.5\,\mathrm{kV\,cm}^{-1}$). The remanent polarization for $BaTiO_3-SiO_2$ is smaller than in pure, sol–gel derived $BaTiO_3$. This is due to the presence of SiO_2 as a dielectric matrix which separated the ferrons. However, the fact that a remanent polarization is observed is a clear indication that dipoles in the ferrons are able to interact with each other.

It should be pointed out that such an interaction is probably possible because the matrix separating the dipoles is a mixture of amorphous silica and still amorphous ferroelectric. The space between the ferrons is filled with a still large fraction of amorphous $BaTiO_3$ or $LiNbO_3$. At 200 °C, ferrons represent only a small fraction of the 50 mole percent present in the original solution. Most of the Ti–O octahedra, for example, are present in the structure in an amorphous phase not detectable via high-resolution TEM (HRTEM) or x-ray diffraction. The distorted Ti–O and Nb–O octahedra which separate the ferrons can contribute to an interaction between ferrons too far apart for a direct interaction.

P–E hysteresis loops were also observed in the ternary $BaTiO_3-TDP-SiO_2$ and $LiNbO_3-TDP-SiO_2$ systems, which were only cured at 200 °C for 2 h. They are shown in

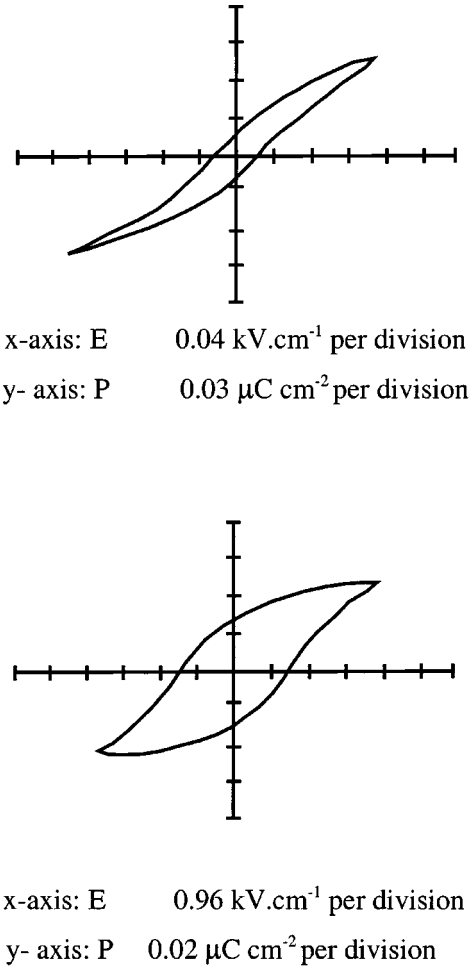

FIG. 3. P–E loops in 45% TDP-45% $LiNbO_3$–$10SiO_2$ (top) and 45% TDP-45% $BaTiO_3$–$10SiO_2$ (bottom) heat treated at 200 °C for 2 h.

Fig. 3. These were observed in spite of the presence in the structure of the materials of a large fraction of organics which may contribute to conduction processes. These loops show that the materials contain dipoles, and that these dipoles are able to align reversibly under an electric field. It is difficult, however, to saturate the alignment of the dipoles. This is reflected in the shape of the loops, which are symmetrical but do not reach horizontality at high fields. In fact, when higher fields were applied across the films, the loops did tend to exhibit a semi-conducting nature (i.e., *P* would increase significantly as a function of *E*).

The spontaneous polarization of the $45LiNbO_3$–$45TDP$–$10SiO_2$ samples was 0.44 $\mu C\,cm^{-2}$ and that of a $45BaTiO_3$–$45TDP$–$10SiO_2$ sample was 0.27 $\mu C\,cm^{-2}$. (Figs. 4 and 5). The $BaTiO_3$–TDP–SiO_2 sample, as expected, had a higher coercive field. It was also found that it was possible to align the TDP dipoles in a $10SiO_2$–$90TDP$ sample, but that the coercive field necessary to do was quite high (20 $kV\,cm^{-1}$).

B. Optical properties

Films of all compositions, spun on quartz substrates, were transparent after firing at 200 °C. Although the $BaTiO_3$–SiO_2 and the $LiNbO_3$–SiO_2 compositions were colorless, the TDP-doped samples were colored. The TDP–$LiNbO_3$–SiO_2 samples exhibited the characteristic yellow color of TDP with a maximum of absorption at around 350 nm. The TDP–$BaTiO_3$–SiO_2 samples were red. Figure 5 shows that the TDP–$BaTiO_3$–SiO_2 samples exhibit an additional absorption peak at around 520 nm. This color change is not observed with the lithium–niobium double alkoxide. The color change occurs upon mixing in the solution and is maintained through the gelation into the heat-treated material. Preliminary studies have shown that the intensity of the absorption peak at 520 nm varies as a function of the TDP/Ba ratio, and is maximal for a TDP/Ba ratio of 1. Similar color changes have also been observed when TDP is mixed with other organo–metallic compounds such as cerium, lanthanum methoxywthoxide, tin isopropoxide, and various other alkoxides. The color change is most likely due to a Lewis base interaction between the amine group in the TDP and the empty orbitals of the metal, which leads to a perturbation of the system of delocalized electron in the TDP molecule.

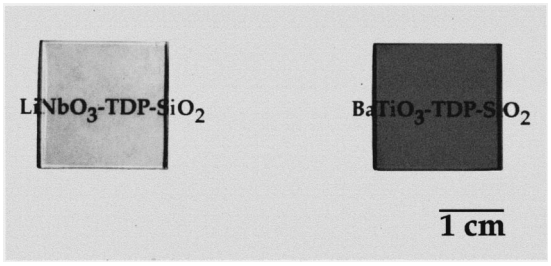

FIG. 4. Color change for TDP-doped ferroelectric films on quartz substrates.

Using a technique described by Kim *et al.*,[8] it was shown that it is possible to orient the TDP molecules in the direction of an external electric field. Using a corona poling field of 10 kV/cm applied at 90 °C, it was possible to align about 30% of the TDP molecules in the direction of the applied electric field, or 20% in the case of TDP–$LiNbO_3$–SiO_2 or TDP–$BaTiO_3$–SiO_2, which was reflected in a decrease in the absorption maxima under polarized light. This illustrates the possibility of inducing noncen-

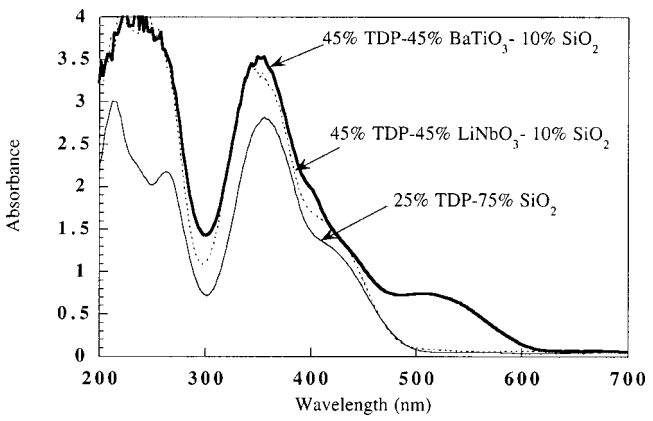

FIG. 5. Spectral characteristics of TDP–SiO_2, TDP–$LiNbO_3$–SiO_2, and TDP–$BaTiO_3$–SiO_2.

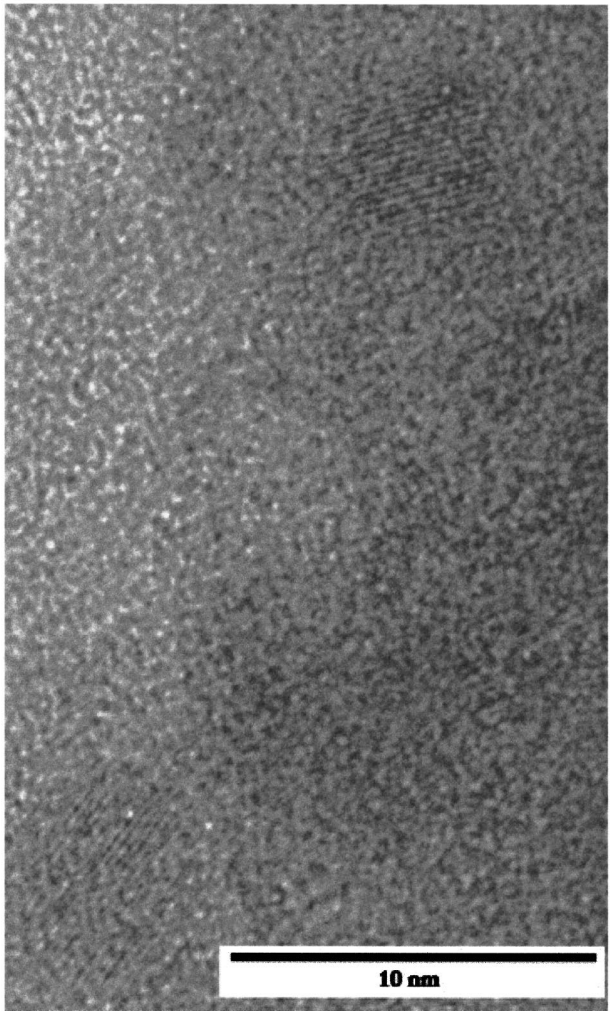

FIG. 6. Ferrons in $LiNbO_3$–SiO_2, heat treated at 200 °C.

trosymmetry in the materials, and demonstrates their potential usefulness as a nonlinear optical media.[9]

C. Microstructures

HRTEM investigation of the $LiNbO_3-SiO_2$ and $BaTiO_3-SiO_2$ mixtures, heat treated at 200 °C for 200 °C revealed the presence of small, ordered clusters of crystalline materials, dispersed throughout an amorphous matrix. Figure 6 shows a typical microstructure for a $LiNbO_3-SiO_2$. Such small crystallites have previously been observed in single phase, sol–gel derived $BaTiO_3$ or $LiNbO_3$.[10] Electron diffraction of such small crystals revealed a tetragonal crystal structure for the ferrons observed in $BaTiO_3-SiO_2$ and a hexagonal crystalline structure for the ferrons observed in $LiNbO_3-SiO_2$, for materials heat treated at 400 °C. These are single crystals. Figure 7 shows that the ferrons are also observed in the TDP-doped materials.

At 200 °C, however, materials were amorphous by x-ray diffraction, as shown in Fig. 8. Crystallinity by x-ray diffraction does not develop clearly until 700 °C for $LiNbO_3-SiO_2$ mixtures, or 300 °C for pure $LiNbO_3$. Figure 8 also shows the delay in crystallization temperature observed when the

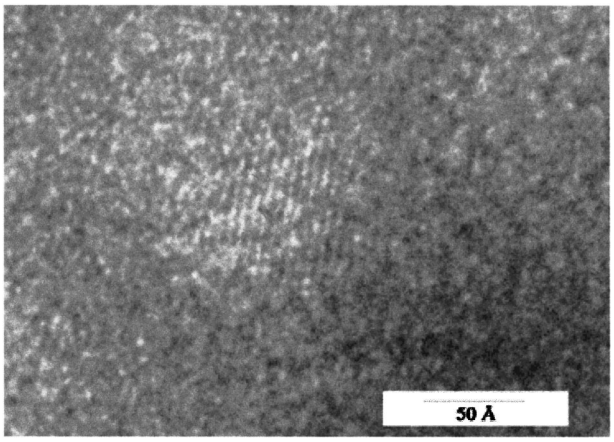

FIG. 7. Ferrons in TDP–$LiNbO_3$–SiO_2, heat treated at 200 °C.

pure $LiNbO_3$ is diluted with SiO_2. A dilution of 50 mole percent results in a delay in crystallization of about 400 °C for $LiNbO_3$.

It is interesting to note that the ferroelectric phases are the only ones to crystallize from the amorphous SiO_2 matrix, and that no ''foreign'' phases such as Li_2O, TiO_2, or BaO, etc., are formed. It has been established already that the structures of any double alkoxides such that the local environment of the metals in the alkoxides is very similar to that of the final oxide, leading to low crystallization temperatures.

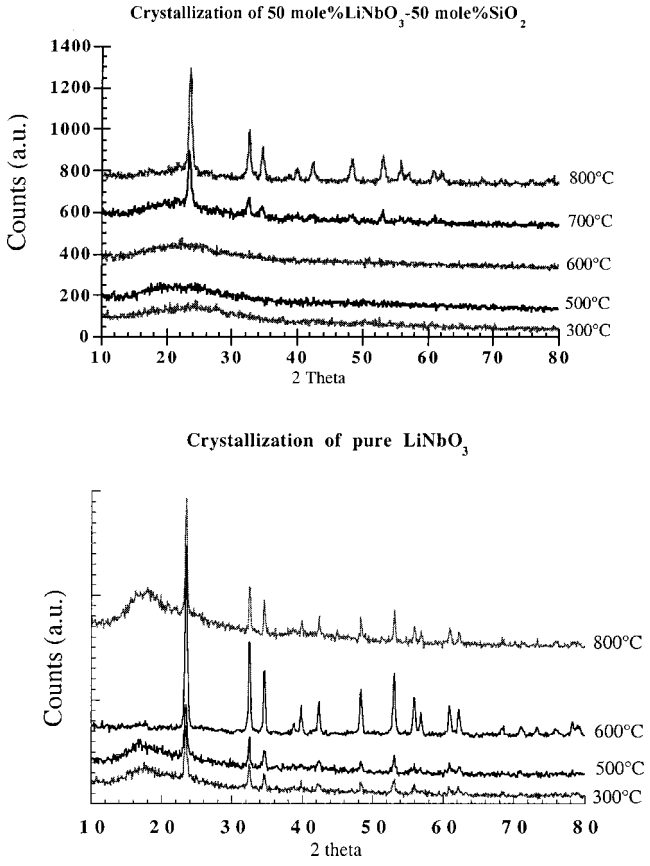

FIG. 8. Crystallization of $LiNbO_3$ in silica (top) compared to the crystallization of pure $LiNbO_3$ (bottom).

These materials are good representatives of two new classes of materials. In the first class, a ferroelectric is dispersed in an amorphous inorganic matrix. The material is transparent and behaves as a weak ferroelectric. This concept may perhaps be extended to other oxides such as ferromagnetic or semiconducting oxides.

In the second class of materials, the ferroelectric phase is now embedded in an organically modified matrix. The organic modification may involve a covalently-attached optically active molecule (such as TDP), a molecule with high hyperpolarizability, a liquid crystal, a conducting polymeric chain, or even an organic chain which would improve the mechanical properties of the composite. The organic modification may also be applicable to other inorganic phases (ferroelectric, ferromagnetic, semiconducting, etc.) and may lead to interesting phenomena as is the case with the TDP–$BaTiO_3$ combination.

IV. THEORETICAL UNDERSTANDING

In order to explain the observation of P–E loops in these multiphase materials, it is necessary to extend a previously published theoretical treatment explaining the interactions between dipoles in sol–gel derived ferroelectrics such as $Pb(Zr_xTi_{1-x})O_3$ (PZT) and $BaTiO_3$. The following treatment may be applied to many ferroelectric oxides such as $LiNbO_3$ or $BaTiO_3$ previously discussed.

A. Ferron model and calculation

In a previous paper[11] we reported experimental results on amorphous thin films of $Pb(Zr_xTi_{1-x})O_3$ (PZT) and $BaTiO_3$ prepared by the sol–gel technique. The most important finding is that amorphous PZT and $BaTiO_3$ thin films exhibit **P**–**E** hysteresis loop, stable pyroelectric current, and piezoelectric resonance peaks in dielectric spectrum. This ferroelectric-like properties indicate that there is a permanent polarization, which can be reversed by an external field, in the amorphous PZT and $BaTiO_3$ films. In addition, the microstructure of the film showed the presence of ''ordered'' group which we named ferrons in amorphous matrix. The ferrons have typical dimension of 3–5 nm. A ferron can be regarded as a nanocrystallite with aligned electric dipoles. These ferrons are separated from one another by disordered regions but apparently can give rise to long-range interactions to produce permanent dipoles. Obviously, the advantages of ferroelectric-like amorphous materials are low processing temperatures, low dielectric permittivity and good transparency without grain boundaries.

From the HRTEM pictures of amorphous PZT films,[11] we observe that there are many small ordered clusters (with the average size between 3 to 5 nm) distributed in a disordered matrix. These ordered clusters are called ferrons. The volume fraction of ferrons to matrix approximates 10%. Ferrons could be distinguished clearly in amorphous HRTEM picture due to their partially ordered pattern. In an amorphous ABO_3 oxides, this ordered structure consists of distorted BO_6 (e.g., TiO_6) octahedra with permanent dipole moment. From experimental results, it has been identified that,[12,13] there are some permanent dipoles, which should be the distorted Ti–oxygen octahedra and Zr–oxygen octahedra, in the network of amorphous structure. An example is $BaTiO_3$ prepared from metal alkoxides.[14] It is likely that some short range order formed during gelation. After heat treatment, the water and the organic, are evaporated, and an amorphous film with a random network is formed. In our previous paper,[11] we discussed that in all the systems the most stable state is $BaTi_4(OR)_{18}$ entity which is similar to a cell of crystalline $BaTiO_3$ but not symmetrical. When this amorphous film is further heated near 400 °C, some small, ordered clusters (ferrons) form. If the heat treatment temperature is controlled below the temperature of the formation of embryos in the amorphous matrix, e.g., 400 °C in our case, nucleation should not happen.

As reported in our paper,[11] the most important finding is that amorphous PZT and $BaTiO_3$ thin films exhibit **P–E** hysteresis loop and stable pyroelectric current. These ferroelectric **P–E** hysteresis loops indicate that there is a permanent polarization, which can be reversed by an external field, in the amorphous PZT and $BaTiO_3$ films.

The peaks observed in the dielectric spectrum[11] were caused by piezoelectric resonance effects. These resonance peaks have been described in several references for crystalline $BaTiO_3$ and $PbTiO_3$ glass-ceramics samples.[15–18]

Traditional beliefs are that ferroelectricity exists only in crystalline materials but not in amorphous materials. In order to understand the experimental results, i.e., the ferroelectric-like properties of amorphous ferroelectrics, a theoretical explanation is needed. A proper theory can answer following questions: Are the experimental results really contrary to the classical theory of ferroelectricity? What is the origin of the ferroelectric-like properties in amorphous ferroelectrics? Is it possible to develop amorphous ferroelectric materials? A theoretical model (ferrons model) is needed, based on experimental observations, to attempt to give some solutions to these questions. A statistical physics approach in accordance with the above ferron model has been used for calculation.

1. Statistically averaged dipole moments and Lorentz correction

Based on the ferrons observed in HRTEM patterns, we propose an independent system consisting of ferrons separated by a distance large comparable to ferron dimensions, so that the ferron system can be seen as an independent system without interaction. Therefore, the energy of the ferron system can be calculated by using a Boltzmann distribution law.[16] Every ferron may have a net dipole moment which is caused by the distortions from the prototypic BO_6 octahedral unit, and the contribution of A^{2+} cations (Ba, Pb) is very small[13] and can be neglected. In this model the magnitude and direction of dipole moment in each ferron may differ, as shown in Fig. 9(a). However, we can consider, mathematically, that each dipole moment consists of some basic dipole moments with the same magnitude of a dipole moment of a BO_6 octahedral unit, $\boldsymbol{\mu}_F$, but with differing directions. A basic dipole moment should be the dipole moment of a unit cell in ferroelectric crystal. Since the dipoles in a ferron differ from the dipoles in crystals, the ferroelectric-like amorphous material can be treated as an ensemble of many randomly oriented dipoles.

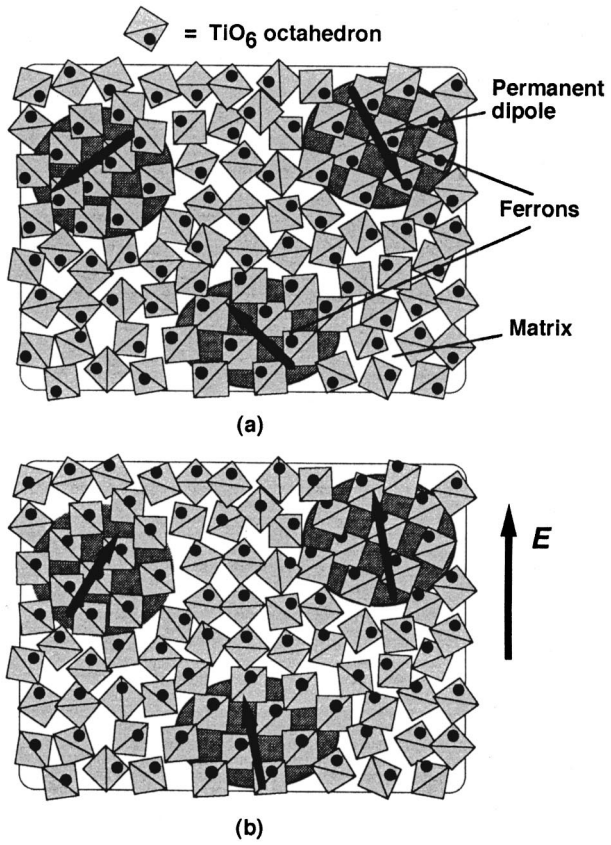

FIG. 9. Illustration for poling ferrons in amorphous ferroelectric thin film. (a) Before poling dipoles are random and (b) After poling dipoles are preferentially oriented.

When the system which contains randomly oriented dipoles $\boldsymbol{\mu}_F$ is in a thermal equilibrium state at room temperature without an external field, the thermally averaged value of dipole moments is zero. When a field $\mathbf{E}$ (assume $\mathbf{E}$ is along the z axis) is applied, these dipole moments are poled and oriented preferentially, as shown in Fig. 10(b). If θ is the angle between the z axis and $\boldsymbol{\mu}_F$, the component of the dipole moment in the z direction is $\boldsymbol{\mu}_z = \boldsymbol{\mu}_F \cos\theta$. Based on Langevin and Debye's theories,[16] the thermally averaged value of dipole moments is

$$\langle \boldsymbol{\mu}_z \rangle = (\boldsymbol{\mu}_F^2/3kT)\mathbf{E}, \tag{1}$$

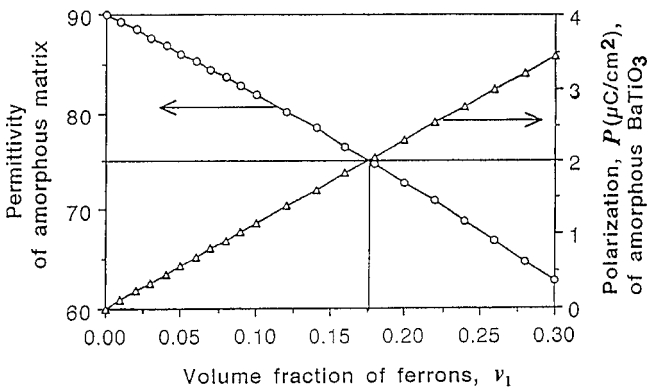

FIG. 10. Graphic solution for volume fraction of ferrons, permittivity of matrix, and polarization of amorphous $BaTiO_3$.

where k is Boltzmann's constant ($=1.380\,662\times10^{-23}$ J/K), and T is the absolute temperature. The field $\mathbf{E}$ in Eq. (1) should be a local field, $\mathbf{E}_L$. We assume that the electrical interaction between the dipoles of ferrons is very small so that a ''Lorentz correction'' can be used, i.e., $\mathbf{E}_L$ is equal to the external field $\mathbf{E}_{\text{appl}}$ plus a ''Lorentz correction factor'':

$$\mathbf{E}_L = \mathbf{E}_{\text{appl}} + \mathbf{P}_a/3\epsilon_0, \tag{2}$$

where $\mathbf{P}_a$ is the polarization of other poled molecules around a $\boldsymbol{\mu}_F$, and ϵ_0 is the electric permittivity of vacuum. Combining Eqs. (1) and (2), we have

$$\langle \boldsymbol{\mu}_z \rangle = (\boldsymbol{\mu}_F^2/3kT)\mathbf{E}_c[(\epsilon_{r(a)}+2)/3], \tag{3}$$

where $\epsilon_{r(a)}$ is the permittivity of the amorphous matrix. Equation (3) is a basic equation for calculating $\langle \boldsymbol{\mu}_z \rangle$, an average of the dipole moment for BO_6 octahedral unit, by a statistical physics approach.

Further, if N is the number of BO_6 octahedral units per unit volume of sample, according to the basic definition of polarization,[19] we have

$$\mathrm{P} = N\langle \boldsymbol{\mu}_z \rangle.$$

Assuming that the density of a ferron is approximately equal to ρ, the density of the polycrystalline material having the same composition, N can be calculated from the formula

$$N = \rho \times N_A / W_{\text{mol}}, \tag{4}$$

where N_A is Avogadro's number ($=6.022\,045\times10^{23}\,\text{mol}^{-1}$), and W_{mol} is one mole weight of the compound.

The remanent polarization $\mathbf{P}_r$ of an amorphous ferroelectric film can be calculated as follows:

$$\mathbf{P}_r = N v_1 \langle \boldsymbol{\mu}_z \rangle, \tag{5}$$

where v_1 is the volume fraction of ferrons.

2. Dielectric permittivity of a two phase material

According to the ferron model of amorphous metal oxides, a macroscopic property of the material can be calculated using a mathematical method, as in the case of a particulate composite. Based on Maxwell–Wagner effect[14,18] the dielectric permittivity of two phase mixture materials can be expressed as follows:

$$\epsilon_r^n = v_1\epsilon_1^n + v_2\epsilon_2^n \quad (-1 \leqslant n \leqslant +1), \tag{6}$$

where the index $n=1$ corresponds to the extreme case of ''parallel connectivity,'' and $n=-1$ corresponds to the extreme case of ''series connectivity,'' ϵ_r is the dielectric permittivity of the overall two-phase material, ϵ_1 and ϵ_2 are the permittivities of both phases (i.e., ferrons and matrix), respectively, v_1 the volume fraction of ferrons, and $v_2(=1-v_1)$ the volume fraction of matrix. Each term in Eq. (6) can be expanded as the form of a power series of ''A^x.'' If n is small, the square term and higher power terms can be neglected, thus, we have

$$\ln \epsilon_r = v_1 \ln \epsilon_1 + v_2 \ln \epsilon_2. \tag{7}$$

The above formula is call the ''logarithmic mixture rule'' [14] and is one of the basic equations in this theoretical calcula-

tion. In this equation the permittivity of the overall thin film, ϵ_r, is an experimental result, and ϵ_1 is the permittivity of a ferron which should be approximately equal to that of a polycrystalline film of the same composition. Equation (7) can be rewritten as

$$\epsilon_2 = \exp[(\ln \epsilon_r - v_1 \ln \epsilon_1)/(1-v_1)]. \quad (8)$$

3. Solution for the volume ratio of ferrons

Examining the experimental data in Ref. 11, the dielectric permittivity of amorphous piezoelectric transducer (PZT) and $BaTiO_3$ is less than that of crystalline PZT and $BaTiO_3$. Amorphous films have smaller permittivity, smaller remanent polarization, and smaller pyroelectric coefficients than those of polycrystalline films with the same composition. This is understandable, because there is only a small volume fraction (estimated around 10 volume % from HRTEM image) of the ordered structure in the amorphous samples. However, the volume fraction of ferrons, v_1, is not easily obtained from the HRTEM image because the image is that of only a small region $\sim 0.1\,\mu\text{m} \times 0.1\,\mu\text{m}$.

To obtain the v_1, a graphic method is used. The graphic method includes (1) plotting the curve of ϵ_2 as a function of v_1 from Eq. (8), (2) plotting the curve of $\mathbf{P}_r$ as the function of v_1 from Eq. (5), (3) combining $\epsilon_2(v_1)$ and $\mathbf{P}_r(v_1)$ curves into a double lines graphic with same horizontal axis of v_1, and (4) solutions for v_1, ϵ_2, and $\mathbf{P}_r$ can be obtained from the point of intersection of the two curves. The two basic equations are repeated:

$$\mathbf{P}_r = N v_1 \langle \boldsymbol{\mu}_z \rangle, \quad (9)$$

$$\epsilon_2 = \exp[(\ln \epsilon_r - v_1 \ln \epsilon_1)/(1-v_1)]. \quad (8)$$

By substituting the experimental data listed in Ref. 11 into Eqs. (8) and (9), we obtain two sets of $\mathbf{P}_r(v_1)$ and $\epsilon_2(v_1)$ equations for amorphous ferroelectric materials. For calculation, we take amorphous $BaTiO_3$ as an example.

4. Calculation for amorphous $BaTiO_3$ film

The weight per mole of $BaTiO_3$, $W_{\text{mol}} \sim 233.21 \pm 0.05$ g/mol. The density of $BaTiO_3$ bulk ceramic can be taken approximately as the density of ferron, $\rho \sim 5.7 \pm 0.05\,\text{g/cm}^3$. Substituting the above data in to Eq. (4), the number of BO_6 octahedral unit per cm^3 in $BaTiO_3$ ferron can be calculated to be approximately $1.47 \pm 0.001 \times 10^{22}/\text{cm}^3$. We assume the density of a ferron to approximate that of the polycrystalline ceramic. Therefore, the dipole moment of BO_6 octahedra unit in $BaTiO_3$ ferron, $\boldsymbol{\mu}_F$ should approximate the dipole moment unit of the corresponding ceramic. If the remanent polarization of bulk ceramic $BaTiO_3$, $\mathbf{P}_r = 26 \pm 0.5\,\mu\text{C/cm}^2$ (in Ref. 11), is taken instead of that of the polycrystalline film, we then have

$$\boldsymbol{\mu}_F = \mathbf{P}_r/N \sim (26 \pm 0.5 \times 10^{-6}\,\text{C/cm}^2)/(1.47 \pm 0.001 \times 10^{22}/\text{cm}^3) \sim 17.7 \pm 0.4 \times 10^{-28}\,\text{C cm},$$

and thus

$$\boldsymbol{\mu}_F^2 \sim 312 \pm 14 \times 10^{-56}\,\text{C}^2\,\text{cm}^2.$$

Substituting this value of μ_F^2 into Eq. (3), and taking $3kT\,(\text{at } T = 300\,\text{K}) = 1.24 \pm 0.001 \times 10^{-20}\,\text{J} = 1.24 \pm 0.001 \times 10^{-20}\,\text{V C}$, $\epsilon_{r(a)}$ (of the overall amorphous sample) $= 90 \pm 2$ (at 1 kHz), and $\mathbf{E}_c \sim 1.1 \pm 0.2 \times 10^5$ V/cm, the statistically averaged value of the dipole moment of BO_6 octahedra unit in $BaTiO_3$ ferrons from the Eq. (3) is

$$\langle \boldsymbol{\mu}_z \rangle_{\text{BT}} = (\boldsymbol{\mu}_F^2/3kT)\mathbf{E}_c[(\epsilon_{r(a)}+2)/3] \sim (3.12 \pm 0.14 \cdot 10^{-54} \times 1.1 \pm 0.2 \cdot 10^5 \times 31 \pm 1)/(1.24 \pm 0.001 \times 10^{-20}) \sim 7.8 \pm 0.8 \times 10^{-28}\,(\text{C cm}).$$

Finally, from Eq. (5), we have

$$\mathbf{P}(v_1) = N \times v_1 \times \langle \boldsymbol{\mu}_z \rangle_{\text{BT}} \sim v_1 \times 11.5 \pm 1.2 \times 10^{-6}\,\text{C/cm}^2. \quad (9a)$$

Equation (9) will be plotted in order to obtain a graphic solution.

Another curve for the graphic solution is obtained from Eq. (8), taking the permittivity of overall amorphous $\epsilon_r = 90 \pm 2$ and that of ferron $\epsilon_1 = 210 \pm 5$ (to approximate polycrystalline $BaTiO_3$ film), i.e.,

$$\epsilon_2 = \exp[(\ln \epsilon_r - v_1 \ln \epsilon_1)/(1-v_1)] = \exp\{[\ln(90 \pm 2) - v_1 \ln(210 \pm 5)]/(1-v_1)\} \sim \exp(4.5 - v_1 \times 5.35)/(1-v_1). \quad (8a)$$

Using v_1 as the variable on the horizontal axis, with values from 0.00 to 0.30, the corresponding value of $\epsilon_2(v_1)$ and $\mathbf{P}_r(v_1)$ can be calculated and scaled on two vertical axes with adding boundary condition, $\mathbf{P}_r = 26 \pm 0.5\,\mu\text{C/cm}^2$ ($v_1 = 1$); we obtain two curves as shown in Fig. 10. Consequently, solutions for v_1, ϵ_2, and $\mathbf{P}_r$ can be obtained from the point of intersection of the two curves. The result is:

$$v_1 = (17.6 \pm 0.3)\%, \quad \epsilon_2 = 75 \pm 1,$$

and

$$\mathbf{P}_r = (2.1 \pm 1)\,\mu\text{C/cm}^2.$$

They are very close to the experimental data in Ref. 11.

For $BaTiO_3$–SiO_2 materials, the model also explains the observed ferroelectric properties, and the addition of SiO_2 merely leads to a dilution of the dielectric constant. One may undertake similar calculation taking into consideration the dielectric constant of a $BaTiO_3$ ferron (90), the dielectric constant of amorphous $BaTiO_3$ (210), and the dielectric constant of SiO_2.[4] Assuming that about 10 vol. % of the BaTiO3 is found in the materials as ferrons, the dielectric constant of the BaTiO3 component of the material is $\epsilon_{\text{BaTiO3}} = 98$. The dielectric constant of the $BaTiO_3$–SiO_2 mixture, assuming a 1:1 molar ratio hence 40 vol % SiO2- 60 vol % $BaTiO_3$, is $\ln \epsilon_{\text{BaTiO3+SiO2}} = 0.4 \ln 4 + 0.6 \ln 98 = 27$. Taking into account the porosity of the material around 50 vol % (since the materials have not been heat treated above 200 °C), the total permivittivity of the mixture is $\epsilon_{\text{total}} = 5.19$. Although the molar ratio of $BaTiO_3$–SiO_2 is 1, the dielectric constant remains very close to that of SiO_2.

A theoretical remanent polarization for a $50BaTiO_3$–$50SiO_2$ sample can easily be calculated using the model. Assuming that 10 vol %. of the $BaTiO_3$ can be found

as ferrons, a porosity of 50%, the total ferron volume in the material is 2%. Hence, the theoretical remanent polarization is $P_r = 0.2\,\mu C\,cm^{-2}$. This value is in excellent agreement with the experimental value of $0.24\ \mu C\,cm^{-2}$ for $BaTiO_3$–SiO_2 films, as measured above. It must be noted that the effects of organic modification by TDP were not taken into account in the model. It is clear, from the optical characteristics of the films, that there is interaction between TDP and one of the metals of the ferroelectric (Ti or Ba). This interaction might involve partial electron transfer from the TDP to the empty *d* orbitals of the metal. The nature and the extent of this influence are not clear yet, and will require further analysis.

V. CONCLUSIONS

In this article, two new classes of transparent ferroelectrics have been studied. The microstructure of the first class consists of small crystals of ferroelectrics such as $LiNbO_3$ or $BaTiO_3$ dispersed in SiO_2. The microstructure of the second class of materials, consists in the same ferroelectrics crystals dispersed in an organically modified silica matrix. Both classes of materials behave as weak ferroelectrics. The first class of materials can probably be extended to many other ferroelectrics such as PZT, PLZT, $KNbO_3$, etc. or even semiconducting or magnetic oxides small particles in glass. The second class of materials is typical of a new family of ''organically-modified glass ceramics'' in which a small inorganic crystal is grown in an organic–inorganic matrix, where the organic may be optically active, or may be designed to bring flexibility to the structure. Opportunities for the study of interactions between inorganic crystals and organic molecules probaly abound. These two new families of materials also offer exciting prospects as new transparent films for integrated optics and nonlinear optics.

ACKNOWLEDGMENTS

The authors wish to acknowledge the support of the Air Force Office of Scientific Research.

[1] J. D. Mackenzie, in *Ultrastructure Processing of Advanced Ceramics*, edited by J. D. Mackenzie and D. R. Ulrich (Wiley, New York, 1989), p. 589.
[2] Y. H. Xu, C. H. Cheng, Y. D. Lou, and J. D. MacKenzie, Ferroelectrics **195**, 288 (1997).
[3] J. D. Mackenzie, and Y. H. Xu, J. Sol-Gel Sci. Technol. **8**, 673 (1997).
[4] Y. H. Xu, C. J. Chen, R. Xu, and J. D. Mackenzie, Phys. Rev. B **44**, 35 (1991).
[5] X. Ren, Ph.D. dissertation, UCLA, 1991.
[6] E. Bescher, Ph.D. dissertation, UCLA, 1997.
[7] Y. Xu, Ph.D. dissertation, UCLA, 1996.
[8] J. Kim, J. Plawsky, E. Wagenen, and G. Korenowski, Chem. Mater. **5**, 1118 (1993).
[9] B. Lebeau, Ph.D. thesis, Université P. M. Curie, Paris, 1997.
[10] R. Xu, Y. Xu, and J. Mackenzie, Proc. SPIE **1758**, 261 (1992).
[11] X. Yuhuan and J. D. Mackenzie, J. Non-Cryst. Solids **176**, 1 (1994).
[12] C. J. Brinker and G. W. Scherer, *Sol–Gel Science-The Physics and Chemistry of Sol–Gel Processing* (Academic, San Diego, 1990), Chap. 2.
[13] Y. W. Chen, W. G. Klemperer, and C. W. Park, Mater. Res. Soc. Symp. Proc. **271**, 57 (1992).
[14] M. I. Yanovskaya, E. P. Turevskaya, V. G. Kessler, I. E. Obvintseva, and N. Y. Turova, Integr. Ferroelectr. **1**, 343 (1992).
[15] S. Roberts, Phys. Rev. **71**, 890 (1947).
[16] I. Bunget and M. Popescu, *Physics of Solid Dielectrics*, 1st ed. (Elsevier Science, Amsterdam, 1984), p. 316.
[17] G. A. Smolenskii, *Ferroelectrics and Related Materials*, 1st ed. (Gordon and Breach, New York, 1984), p. 443.
[18] M. Wu and P. Zhu, J. Non-Cryst. Solids **84**, 344 (1986).
[19] B. Jaffe, W. R. Cook, Jr., and H. Jaffe, *Piezoelectric Ceramics* (Academic, London, 1971), Chap. 3, pp. 37–43.